Supplementary Information

Li-ion and Na-ion transportation and storage properties in various sized TiO_2 spheres with hierarchical pores and high tap density

Yong Li,‡[ab] Shuan Wang,‡[a] Yan-Bing He,*[a] Linkai Tang,[ab] Yusuf Valentino Kaneti,[a] Wei Lv,[a] Zhiqun Lin,[c] Baohua Li,*[a] Quan-Hong Yang[a] and Feiyu Kang[ab]

[a.] *Engineering Laboratory for the Next Generation Power and Energy Storage Batteries, Graduate School at Shenzhen, Tsinghua University, Shenzhen, 518055, PR China. *E-mail: he.yanbing@sz.tsinghua.edu.cn; libh@mail.sz.tsinghua.edu.cn.*

[b.] *Laboratory of Advanced Materials, Department of Materials Science and Engineering, Tsinghua University, Beijing, 100084, PR China.*

[c.] *School of Materials Science and Engineering, Georgia Institute of Technology Atlanta, GA 30332, USA.*

‡ These authors contributed equally to this work.

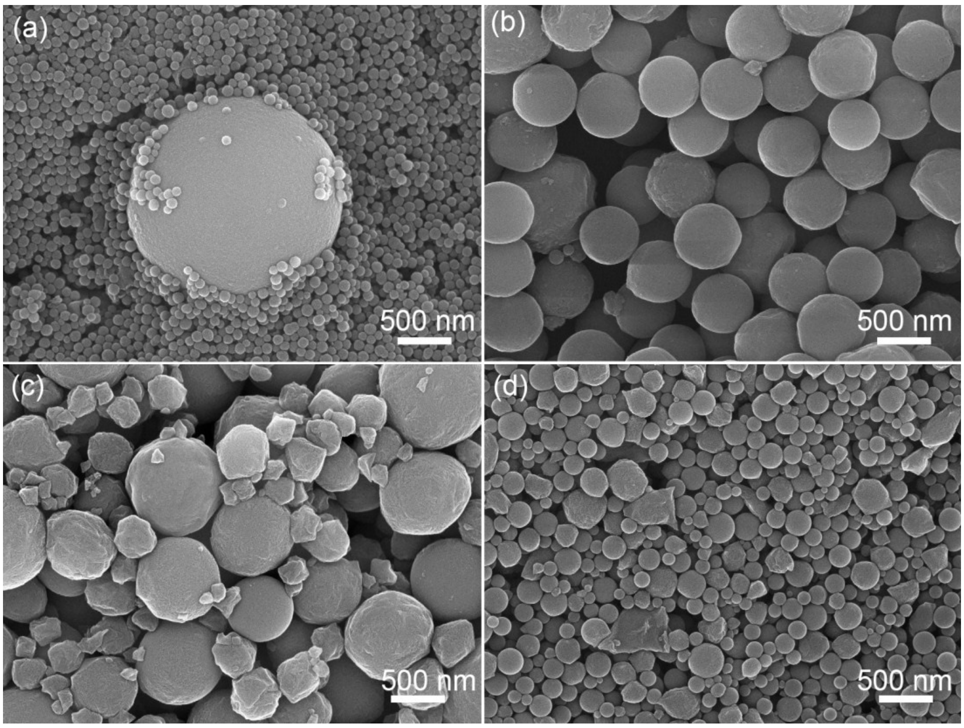
(a)
500 nm
(b)
500 nm
(c)
500 nm
(d)
500 nm

Figure S1. SEM images of amorphous TiO_2 spheres: (a) TiO_2(2:1), (b) TiO_2(1:1), (c) TiO_2(1:2) and (d) TiO_2(1:4). The ratios of the precursor to absolute alcohol in each TiO_2 sphere are shown in the parentheses.

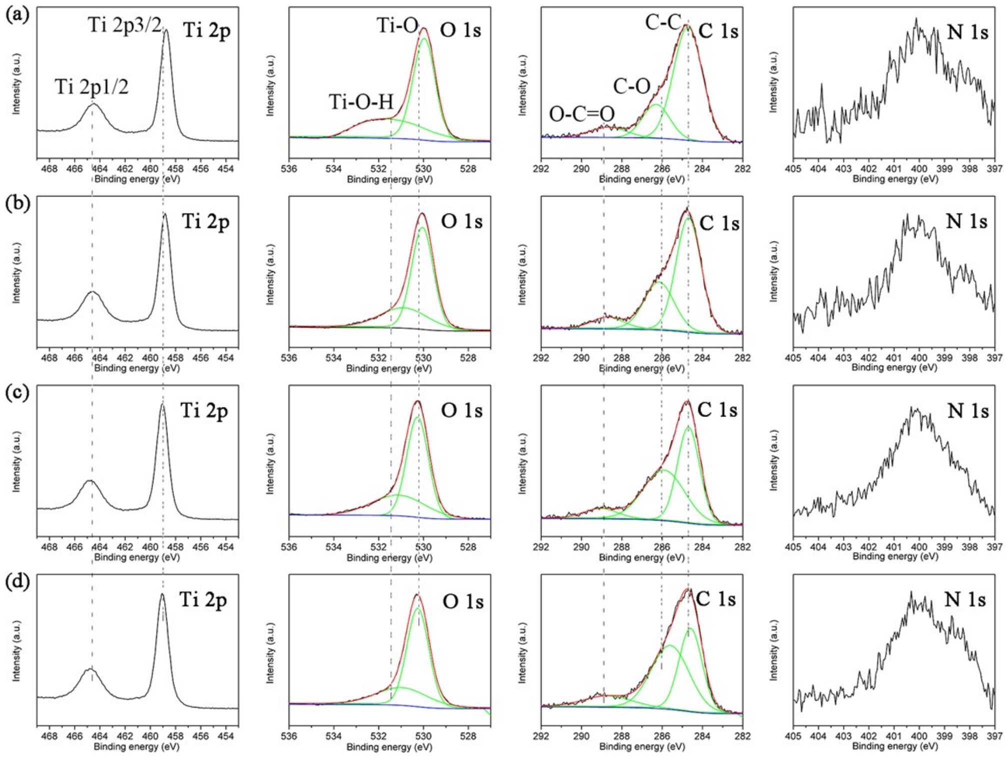

Figure S2. XPS spectra of TiO_2 spheres: (a) TiO_2(2:1), (b) TiO_2(1:1), (c) TiO_2(1:2) and (d) TiO_2(1:4).

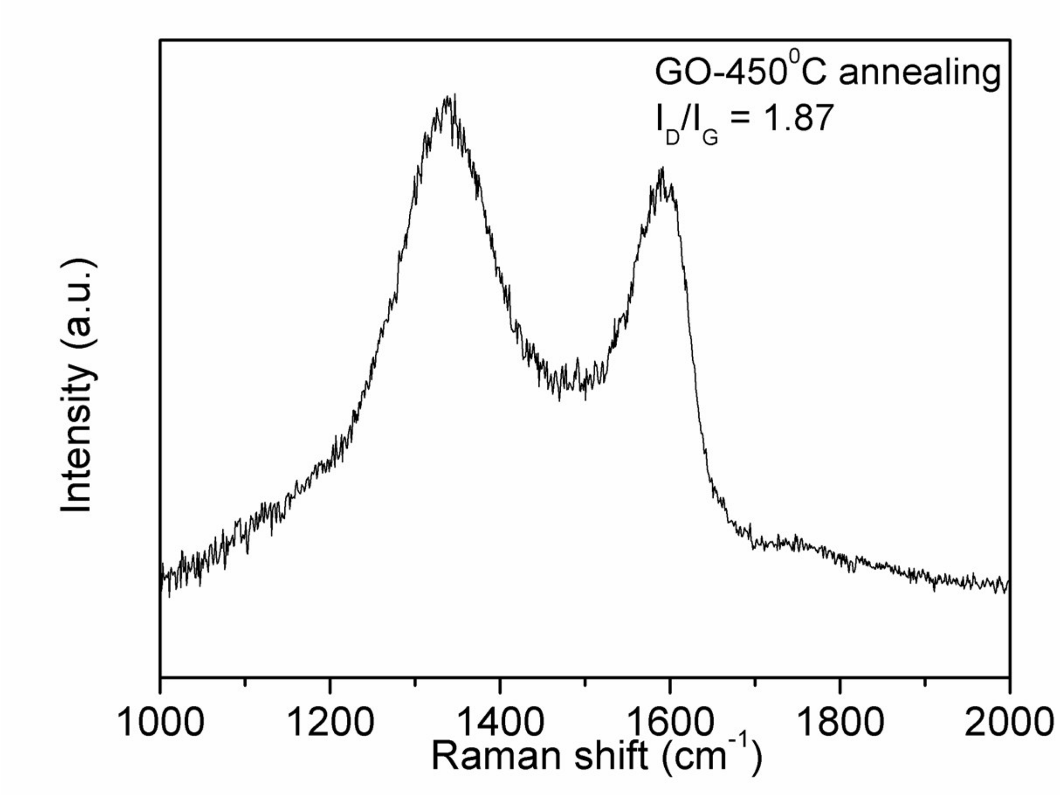

Figure S3. Raman spectrum of graphene oxide annealed at 450 °C.

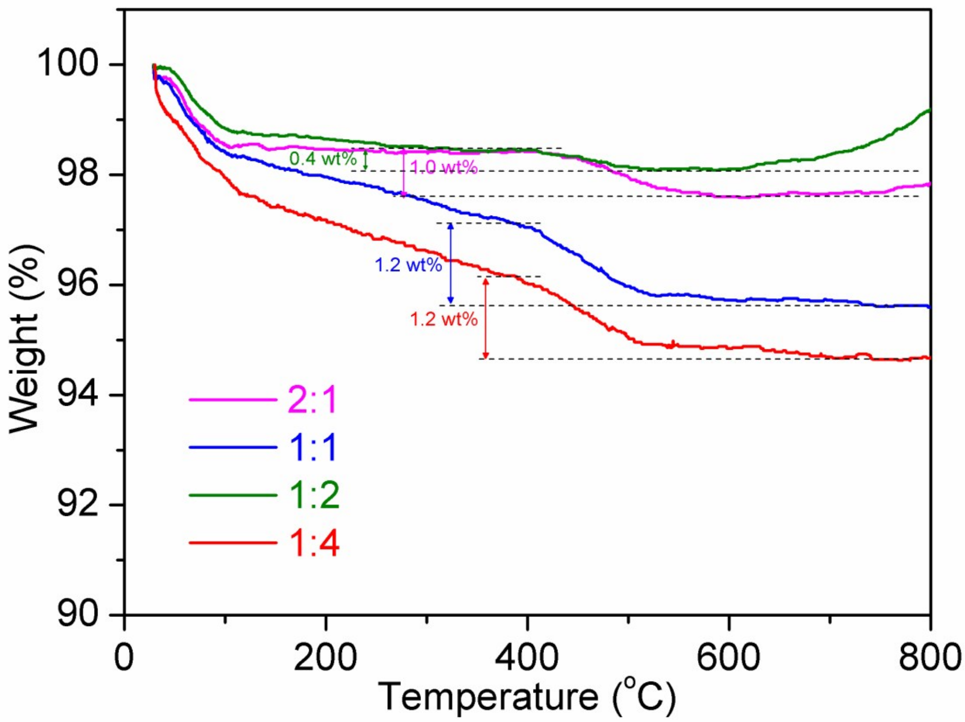

Figure S4. TGA curves of TiO_2 spheres: (a) TiO_2(2:1), (b) TiO_2(1:1), (c) TiO_2(1:2) and (d) TiO_2(1:4).

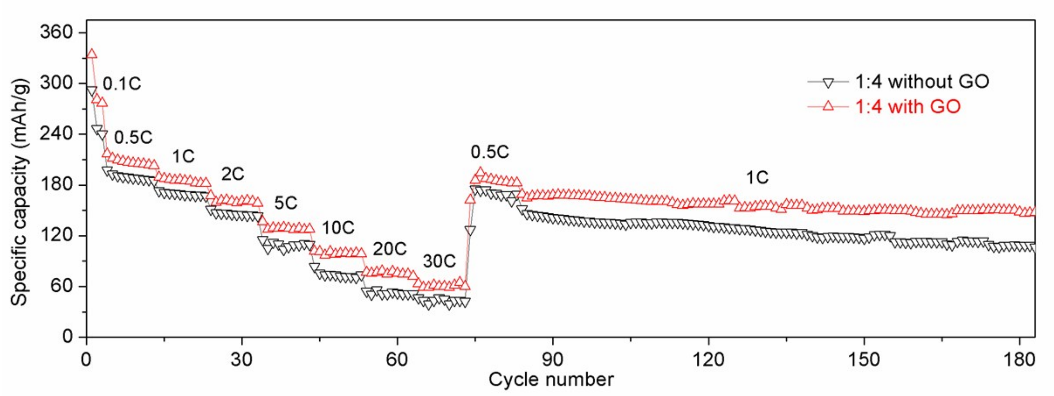

Figure S5. The electrochemical properties of the TiO_2(1:4) electrode with and without the addition of GO.

Calculation of diffusion coefficient

Electrochemical impedance spectroscopy (EIS) measurements were performed to evaluate diffusion coefficient (*D*) through nanospheres. *D* was calculated according to the following equation (1)[1]:

$$D = \frac{R^2 T^2}{2A^2 n^4 F^4 C^2 \sigma^2} \quad (1)$$

where *R* is the gas constant, *T* is the absolute temperature, A is the product of BET surface area and mass of TiO_2 spheres used on the electrode, *n* is the number of electrons transferred in the half-reaction for the redox couple and *F* is the Faraday constant.

C is the concentration of ions, calculated according to the literature[2] and the ion concentration has been calculated in the condition of half lithiated state of TiO_2:

The lithium ion insertion process of TiO_2 is as following:

$$TiO_2 + xLi^+ + xe^- \rightarrow Li_xTiO_2\ (0 \le x \le 1)$$

Since the EIS was measured at half discharge state, thereby, TiO_2 is half lithiated state. Then the C value is calculated according to the following equation (2):

$$C = \frac{\frac{1}{2}\rho}{M} \quad (2)$$

where ρ is the tap density, M is the molar mass.

σ is the Warburg factor, which is related to Z_{re} according to Equation (3), and can be obtained from the slope of $Z_{re} \sim \omega^{-1/2}$ plot as shown in the inset of **Figure 5e** and **6f**.

$$Z_{re} = R_s + R_{SEI} + R_{ct} + \sigma\omega^{-1/2} \quad (3)$$

Table S1. Comparison of electrochemicalperformance of the as-prepared TiO_2 spheres (TiO_2(1:4)) with recently reported literatures for LIBs.

Ref	Synthetic method	Morphology	Carbon content(wt.%)	Capacity(1C)
this work	80°C drying	spheres	3%	180 mAh g^{-1}
[3]	template+hydrothermal	hollow spheres	10.5%	175 mAh g^{-1}
[4]	hydrothermal	nanocrystals	6%	120 mAh g^{-1}
[5]	Hydrothermal	hollow spheres	--	130 mAh g^{-1}
[6]	freeze dry+hydrothermal	nanocrystals	67%	170 mAh g^{-1}
[7]	hydrothermal	microspheres	8.9%	185 mAh g^{-1}
[8]	sol−gel	nanocrystals	48%	170 mAh g^{-1}
[9]	hydrothermal	nanostructure	8%	180 mAh g^{-1}
[10]	hydrothermal	mesocrystals	6.28%	164.9 mAh g^{-1}
[11]	hydrothermal	dendritic	--	151 mAh g^{-1} (0.1 C)
[12]	hydrothermal	hierarchical spheres	20.8%	169 mAh g^{-1}

Table S2. Comparison of the electrochemical performance of the as-prepared TiO_2 spheres (TiO_2(1:4)) with recently reported literatures for SIBs.

Ref	Synthetic method	Morphology	Carbon content(wt.%)	Rate (0.1 C) performance	Cycling performance
this work	80^{o}C drying	spheres	3%	220 mAh g^{-1}	1 C, 195 cycles, 90.5% retention
13	hydrother mal	nanoparticles		~200 mAh g^{-1} (125 mA g^{-1})	125 mAh g^{-1}, 200 cycles, 97% retention
14	template+ ALD	nanoarrays	--	240 mAh g^{-1} (50 mA g^{-1})	50 mA g^{-1}, 50 cycles, 82.9% retention
15	hydrother mal+ template	hollow nanospheres	75%	~250 mAh g^{-1} (50 mA g^{-1})	40 mA g^{-1}, 500 cycles, 72.2% retention
16	hydrother mal	nanoparticles	--	60 mAh g^{-1} (33.5 mA g^{-1})	--
17	sol−gel	--	--	~170 mAh g^{-1} (50 mA g^{-1})	--
18	electrospi nning	nanofibers	1.85%	~205 mAh g^{-1} (67 mA g^{-1})	2 C, 200 cycles, ~90%
19	sol-gel	composite	19.6%	227 mAh g^{-1} (50 mA g^{-1})	50 mA g^{-1}, 50 cycles, ~92.1%
20	hydrother mal	microsphere	6.8%	160 mAh g^{-1}	0.1 C, 50 cycles, ~100%
21	alkyl halide eliminatio	porous composites	45%	~150 mAh g^{-1} (42 mA g^{-1})	42 mA g^{-1}, 50 cycles,

	n				>90%
22	Electron-Beam Melting	nanotube arrays	--	~105 μA cm^{-2} (5 μA)	--

References

1 S. S. Zhang, K. Xu, T. R. Jow, *Electrochim. Acta,* 2004, **49**, 1057.

2 X. Wang, H. Hao, J. Liu, T. Huang, A. Yu, *Electrochim. Acta,* 2011, **56**, 4065.

3 H. Liu, W. Li, D. Shen, D. Zhao, G. Wang, *J. Am. Chem. Soc.,* 2015, **137**, 13161.

4 Z. Zhang, L. Zhang, W. Li, A. Yu, P. Wu, *ACS Appl. Mater. Interfaces,* 2015, **7**, 10395.

5 C. Han, D. Yang, Y. Yang, B. Jiang, Y. He, M. Wang, A.-Y. Song, Y.-B. He, B. Li, Z. Lin, *J. Mater. Chem. A,* 2015, **3**, 13340.

6 B. Qiu, M. Xing, J. Zhang, *J. Am. Chem. Soc.,* 2014, **136**, 5852.

7 X. Yan, Y. Li, F. Du, K. Zhu, Y. Zhang, A. Su, G. Chen, Y. Wei, *Nanoscale,* 2014, **6**, 4108.

8 W. Li, F. Wang, S. Feng, J. Wang, Z. Sun, B. Li, Y. Li, J. Yang, A. A. Elzatahry, Y. Xia, *J. Am. Chem. Soc.,* 2013, **135**, 18300.

9 X. Xin, X. Zhou, J. Wu, X. Yao, Z. Liu, *ACS Nano,* 2012, **6**, 11035.

10 J. Ye, W. Liu, J. Cai, S. Chen, X. Zhao, H. Zhou, L. Qi, *J. Am. Chem. Soc.,* 2010, **133**, 933.

11 Z. Sun, J. H. Kim, Y. Zhao, F. Bijarbooneh, V. Malgras, Y. Lee, Y.-M. Kang, S. X. Dou, *J. Am. Chem. Soc.,* 2011, **133**, 19314.

12 J. S. Chen, Y. L. Tan, C. M. Li, Y. L. Cheah, D. Luan, S. Madhavi, F. Y. C. Boey, L. A. Archer, X. W. Lou, *J. Am. Chem. Soc.,* 2010, **132**, 6124.

13 J.-Y. Hwang, S.-T. Myung, J.-H. Lee, A. Abouimrane, I. Belharouak, Y.-K. Sun, *Nano Energy,* 2015, **16**, 218.

14 Y. Xu, M. Zhou, L. Wen, C. Wang, H. Zhao, Y. Mi, L. Liang, Q. Fu, M. Wu, Y. Lei, *Chem. Mater.,* 2015, **27**, 4274.

15 D. Su, S. Dou, G. Wang, *Chem. Mater.,* 2015, **27**, 6022.

16 M. Søndergaard, K. Dalgaard, E. Bøjesen, K. Wonsyld, S. Dahl, B. Iversen, *J. Mater. Chem. A,* 2015, **3**, 18667.

17 H. Usui, S. Yoshioka, K. Wasada, M. Shimizu, H. Sakaguchi, *ACS Appl. Mater. Interfaces,* 2015, **7**, 6567.

18 Y. Yeo, J.-W. Jung, K. Park, I.-D. Kim, *Sci. Rep.,* 2015, **5**, 13862.

19 C. Fu, T. Chen, W. Qin, T. Lu, Z. Sun, X. Xie, L. Pan, *Ionics,* 2016, **22**, 555.

20 S.-M. Oh, J.-Y. Hwang, C. S. Yoon, J. Lu, K. Amine, I. Belharouak, Y.-K. Sun, *ACS Appl. Mater. Interfaces,* 2014, **6**, 11295.

21 J. Lee, Y.-M. Chen, Y. Zhu, B. D. Vogt, *ACS Appl. Mater. Interfaces,* 2014, **6**, 21011.

22 Z. Bi, M. P. Paranthaman, P. A. Menchhofer, R. R. Dehoff, C. A. Bridges, M. Chi, B. Guo, X.-G. Sun, S. Dai, *J. Power Sources,* 2013, **222**, 461.